Histol Histopathol (2020) 35: 833-847

http://www.hh.um.es

Histology and Histopathology
From Cell Biology to Tissue Engineering

Cathepsin-B dependent autophagy ameliorates steatoheaptitis in chronic exercise rats

Rui Guo[1]*, Qian Yu[1]*, Emily C. Liong[1], Man Lung Fung[1,2] and George L. Tipoe[1,2]

[1]School of Biomedical Sciences and [2]Brain Hormone Healthy Aging Centre,
LKS Faculty of Medicine, The University of Hong Kong, Hong Kong S.A.R.

* These authors have equal contributions.

Summary. Purpose. This study aimed to investigate the role of cathepsin B dependent autophagy induced by chronic aerobic exercise on a high-fat diet (HFD)-induced nonalcoholic steatohepatitis (NASH) in rats. Methods. Healthy female (Sprague-Dawley) SD rats (8-10 weeks old; 180g-200g; n=6 per group) were divided into: (1) control group; (2) HFD group; (3) Exercise group; (4) HFD + exercise group. Rats were fed with a normal chow or an HFD for 12 weeks. Rats with exercise ran on a rotarod for 30 min per day from weeks 9-12. Results. Exercise training significantly (1) upregulated the levels of autophagy markers Beclin1, ATG5 and LC3II partly through inhibiting the p-AKT/mTOR pathway; (2) ameliorated HFD-mediated accumulation of fat mass by upregulating β-oxidation regulator PPAR-α and downregulating fatty acid synthesis marker SREBP-1c via lipophagy; (3) diminished the HFD-induced hepatic pro-inflammatory mediators TNF-α and IL-1β via NF-ϰB inactivation; (4) decreased the NASH-induced hepatic apoptotic marker caspase-3 activation caused by the upstream oxidative stress and by cytochrome P450 2E1 (CYP2E1); (5) mitigated the HFD-mediated lysosomal membrane permeabilisation and cathepsin B release partly via the reduction of reactive oxygen species (ROS). Conclusions. Chronic aerobic exercise reduces oxidative stress/ROS and ROS may cause lysosomal membrane destabilisation and disrupts the autophagic process. The beneficial effect of chronic exercise may further inhibit the process of lysosome membrane permeabilisation and facilitate lysosome fusion with autophagosomes to trigger autophagy. This process may possibly contribute to the inhibition of cathepsin B released into cytosol which further reduces inflammation and mitochondrial-dependent apoptosis.

Key words: Aerobic exercise, Autophagosome, lysosomal membrane, Oxidative stress, Apoptosis

Offprint requests to: George L. Tipoe, School of Biomedica Sciences, LKS Faculty of Medicine, The University of Hong Kong, Hong Kong, S.A.R. e-mail: tgeorge@hku.hk

DOI: 10.14670/HH-18-204

Introduction

Non-alcoholic steatohepatitis (NASH) is the later stage of non-alcoholic fatty liver disease (NAFLD), which is characterised by severe hepatic oxidative stress, inflammation and apoptosis. It could also lead to cirrhosis and hepatocellular carcinoma (Loyer et al., 2016). Autophagy has been demonstrated to have a number of beneficial functions which could prevent NASH development and progression, including decreasing triglyceride and cholesterol accumulation, improving insulin sensitivity, preventing cellular damage from oxidative stress, reducing endoplasmic reticulum stress, and preventing the development of hepatocellular carcinoma (Amir and Czaja, 2011; Lavallard and Gual, 2014; Puri and Chandra, 2014).

Autophagy is a catabolic process that targets cell constituents such as damaged organelles, unfolded proteins, and intracellular pathogens to lysosomes for degradation through fusion of autophagosome with lysosome to form autophagolysosome (Lavallard and

Gual, 2014). It has been reported that autophagy induction by chronic exercise exerted beneficial metabolic effects in protecting hepatocytes against inflammatory diseases such as NASH (He et al., 2012) and NAFLD (Guo et al., 2015). Kim et al., demonstrated that treadmill training promoted age-triggered attenuation of autophagic proteins in mice, which suggested that exercise-induced autophagic response can be considered as a cellular "clearance" mechanism to protect the body system against the accumulation of dysfunctional mitochondria and unfolded proteins (Kim et al., 2013).

Cathepsin B, which acts as a stable protease at physiological pH, has been reported to play an essential role in TNF-α induced liver inflammation and hepatocyte apoptosis in liver steatosis (Alkhouri et al., 2011). In the present study, we initially demonstrated that chronic exercise served as a newly defined stimulus that induced cytoprotective autophagy, which significantly inhibited lysosomal membrane lipids oxidation induced by the upstream ROS, ultimately leading to a reduction of cathepsin B- dependent hepatic oxidative stress, inflammation and apoptosis in NASH. In the present study, oxidative stress is the upstream of cathepsin B. ROS is generated after CYP2E1 catalysis and oxidises lysosomal membrane lipids. Then, cathepsin B is released from lysosome to cytosol. Current knowledge suggests that autophagy occurs via the fusion of autophagosomes and lysosomes. ROS causes lysosomal membrane destabilisation, which disrupts the autophagic process to some extent. Exercise reduces this disruption and facilitates the fusion of autophagosomes and lysosomes. The main aim of this study was to investigate the role of cathepsin B-dependent autophagy induced by chronic aerobic exercise on a high fat diet-induced NASH in Sprague-Dawley rats.

Materials and methods

Reagents

Rabbit anti-cytochrome P450 2E1 (CYP2E1) polyclonal antibody was bought from Millipore (Billerica, MA, USA). Antibodies against PPARα and SREBP-1c were obtained from Santa Cruz Biotechnology (Santa Cruz, CA, USA). Antibodies of Beclin1, LC3, lysosome-associated membrane protein 1 (LAMP1), ATG5, p62, p-AKT, total AKT, p-mTOR, mTOR, VDAC, cytochrome C, COX IV, Bax, cleaved caspase-3, and cleaved poly (ADP-ribose) polymerase (PARP) were purchased from Cell Signaling (Danvers, MA, USA).

Animal experiment

Healthy adult female Sprague-Dawley (SD) rats (8-10 weeks old; 180g-200g) were obtained from the Laboratory Animal Unit (Fully accredited by Association for Assessment and Accreditation Laboratory Care International [AAALAC International]), The University of Hong Kong. They were divided into four groups (n=6 per group) namely: (1) control group (fed with regular rat chow and tap water for 12 weeks); (2) High fat diet (HFD) group (fed with a HFD for 12 weeks); (3) Exercise group (fed with regular rat chow and tap water and trained to run on a rotarod for 30 min per day from weeks 9-12); and (4) HFD + exercise group (HFD feeding for 12 weeks, and running on a rotarod for 30 min per day from weeks 9-12). Exercise intensity consisted of 5m/min for 3 minutes, 10m/min for 3 minutes, and 20 m/min for 24 minutes. All exercising rats completed the prescribed exercise training with no adverse events or major injuries.

The development of NASH in rats, including the protocols for HFD preparation was based on our previously described NAFLD animal model (Tipoe et al., 2009). The diet consists of 9.3 g AIN-93MX (Dyets incorporation, Bethlehem, PA), 2.6 g AIN-93VX (Dyets), 0.5 g choline bitartrate (Dyets), 1.1 g DL-methionine (Bio-serv, Frenchtown, NJ), 57.5 g lactalbulmine hydrolysate (Bio-serv), 117.5 g dextrose (Dyets), 36.6 ml fish oil (Sigma), and 4.5 g suspending agent K (Bio-serv) per 1,000 ml volume. Regular chow for rat (PicoLabH Rodent Diet 20) was purchased from LabDiet (LabDiet, Brentwood, MO). The calories of regular chow were provided by 25% from protein, 13% from fat, and 62% from carbohydrates, while the calories of HFD were provided by 35% from protein, 30% from fat, and 35% from carbohydrates. After twelve weeks, rats were killed by an overdose of anesthesia (150 mg/kg pentobarbital, intraperitoneal injection) according to the protocols approved by the Committee of Animal Use for Research and Teaching at The University of Hong Kong after a 12-hr fasting. Blood and liver samples were collected for further analyses.

Quantitative nuclear magnetic resonance

Body fat mass and composition was measured using quantitative nuclear magnetic resonance (NMR). In the test, rats were individually placed in small tubes and then inserted into a Brucker model mq10 NMR analyzer one at a time (Brucker, Milton, Ontario, Canada). The data of fat mass and composition were recorded within 1 min.

Glucose tolerance test

After 12-week of NAFLD induction, rats were starved for 6 hours with availability of water. Then rats underwent glucose tolerance test (GTT) by intraperitoneally (i.p.) injecting with D-glucose (0.5 g/kg, Sigma-Aldrich, St. Louis, MO). At 0, 20, 40, 60, 80 and 100 min after glucose injection, a tail vein blood sample from each rat was tested for glucose level directly by using ACCU-CHEK blood glucose monitoring system (Roche Diagnostic, Basel, Switzerland).

Tissue and blood samples processing and histological analysis

The blood sera were collected by centrifugation at 1000×g for 10 min at 4°C and stored at -80°C. Liver tissues were fixed in 10% phosphate-buffered formalin for 72 h, processed histologically, embedded in paraffin blocks, cut into 5 μm sections, and stained with haematoxylin and eosin (H&E staining). NASH scoring was also performed on H&E and Sirius Red stained sections (Tipoe et al., 2006).

Serum alanine aminotransferase (ALT) assay

To evaluate the hepatic injury at the enzymatic level, serum ALT level was measured by using ALT (SGPT) reagent set (Teco diagnostics, Anaheim, CA, USA) according to the manufacturer's instructions.

Measurement of malondialdehyde (MDA) level

The malondialdehyde levels were determined using a Bioxytech LPO-586TM kit (Oxis Research, Portland, OR, USA) according to the manufacturer's instructions. Standard curves were constructed using 1,1,3,3-tetraethoxypropane as a standard. The MDA levels were normalised with corresponding protein amounts determined by a Bio-Rad Protein Assay Kit (Bio-Rad, Hercules, CA, USA) and expressed as percentage against the control level.

Preparation of mitochondria and cytoplasmic fractions

Mitochondria and cytoplasmic fractions were prepared using a mitochondrial fractionation kit (Active Motif, CA, USA), according to the manufacturer's protocol. Crude mitochondria were used in this study.

Preparation of cytosolic and membrane fractions

Cytosolic and membrane fractions were prepared using a protein fractionation enrichment kit (Biosciences, PA, USA), according to the manufacturer's protocol.

RNA extraction and quantitative reverse-transcription polymerase chain reaction (Realtime-PCR)

Total RNA was extracted using an illustraTM RNAspin mini kit (GE Healthcare, UK) and then reverse-transcribed with a SuperScriptTM First-Strand Synthesis System (Invitrogen, Calsbad, CA, USA). The mRNA expression levels were measured by a Takara SYBR premix Taq quantitative PCR system (Takara Bio Inc, Shiga, Japan) and in MyiQ2 real-time PCR machine (Bio-Rad) using specific primers as previously described (Kleiner et al., 2005; Tipoe et al., 2009). Parallel amplification of GAPDH was used as the internal control. The relative expression of the specific gene to the internal control was obtained and then expressed as a percentage of the control value in the figures.

Western blot analysis

Cytosolic protein was extracted using a NE-PER protein extraction system (Pierce Biotechnology, Rockford, IL, USA) with the addition of Halt phosphatase inhibitor cocktail (Pierce). Western blotting was performed as previously described (Xiao et al., 2013). The ratio of the optical density of the protein product to the internal control was obtained and levels were expressed as a percentage of the test to the control value using Image J.

Enzyme-linked immunosorbent assay (ELISA)

For NF-κB assay, nuclear extracts were prepared using a NE-PER protein extraction system (Pierce Biotechnology, Rockford, IL, USA). The active NF-κB was then assessed by the level of p65 in the nuclear fractions using an NF-κB/p65-active ELISA kit (Imgenex, San Diego, CA, USA).

TUNEL assay

The terminal deoxynucleotidyl transferase-mediated dUTP-nick end labeling (TUNEL) assay was applied to show the apoptotic cellular damage. It mainly detects 3' hydroxyl ends in fragmented DNA caused by apoptotic signaling cascade. The staining was performed using an in situ cell death detection kit (AP. Roche, USA). DNase I recombinant was used as the positive control. The immunostainings were examined using a light microscope (Zeiss Axiolab, Carl Zeiss Inc. Germany).

Immunofluorescence staining

Frozen sections were blocked with 1% bovine serum albumin, 4% normal goat serum and 1% Triton X-100 for 2h at room temperature. Then, they were incubated with 1:100 dilution of anti-LC3II primary antibody at 4°C overnight. After washing three times with 0.1 M PBS containing 0.5% Triton X-100 for 10 min each time, the sections were incubated with 1:500 dilution of FITC at room temperature for 2 h. Staining was viewed using a fluorescent microscope attached to a DC 200 digital camera (Leica Microsystems Ltd., Heerbrugg, Switzerland).

Assay of cathepsin B activity

Cathepsin B activity was analysed using a cathepsin B activity assay kit (Calbiochem, La Jolla, CA, USA) and using a z-Arg-Arg-AMC as substrate. Activity was determined by measuring fluorescence of free AMC on a fluorescence plate reader at an excitation wavelength of 370 nm and emission wavelength of 450 nm.

Statistical analysis

Data from each group were pooled to generate a mean and a standard deviation. The normality of data distribution was examined by a chi-square test, and group comparisons were performed using One-way ANOVA followed by post-hoc Duncan test. All statistical analyses were performed using SPSS software.

Results

NASH and physical exercise induced cytoprotective autophagy

The protein expression of autophagy markers Beclin1, ATG5, and LC3II was significantly enhanced by HFD-induced NASH as a self-protection mechanism (Fig. 1). Liver samples from the exercise group also showed upregulated Beclin1, ATG5, and LC3II levels. Co-treatment of exercise with HFD did not further increase the levels of autophagy markers (Fig. 1B-D) but they were maintained at a high level. We further investigated the molecular mechanism underlying the induction of hepatic cytoprotective autophagy in chronic exercise. Autophagy activated by both HFD and exercise was partially induced through the inhibition of mTOR activity by downregulating the phospho-mTOR level. NASH induced by HFD as well as chronic exercise remarkably decreased the levels of the phosphorylated form of mTOR, indicating an induction of autophagy after NASH progression and aerobic exercise via the inhibition of mTOR activity. As the upstream of phospho-mTOR, the phosphorylation level of AKT (p-AKT) was not diminished by exercise when compared with control, suggesting that p-AKT may also participate in other signaling pathways, such as apoptosis, to play an important role in the interaction with pro-apoptotic proteins (Fig. 1E,F). The fluorescence staining with LC3II (Fig. 2A) with statistical analysis (Fig. 2B), where the presence of bright green dots suggested an early stage of LC3 aggregation in autophagosomes, correlated with the western blotting results (Fig. 1A), which showed an increase of LC3 content in HFD group, Exercise group and HFD+exercise group.

Exercise reduced NASH-induced lipid accumulation and glucose metabolism dysfunction

After 12 weeks, the mean body weight of HFD-induced NASH rats was significantly higher than that of the control. In the exercise rats from weeks 9 to 12, there was a significant decrease in body weight (Fig. 3A). In addition, dysregulated glucose metabolism in HFD rats was also corrected by exercise indicating an improvement in glucose tolerance (Fig. 3B). For fat mass and fat composition, HFD feeding eventually caused fat accumulation in NASH induced by HFD rats which was alleviated by chronic exercise (Fig. 3C,D). The therapeutic effects of aerobic activity on HFD-induced lipid accumulation were mainly associated with upregulation of lipolytic signaling pathways. NASH induced by HFD significantly reduced the protein expression level of β-oxidation regulator peroxisome proliferator-activated receptor alpha (PPAR-α), which was elevated after chronic physical exercise (Fig. 3E). On the contrary, the level of fatty acid synthesis marker, sterol regulatory element-binding transcription factor 1c (SREBP-1c), was markedly diminished after chronic exercise training (Fig. 3F,G) including in the co-treatment group (HFD + exercise).

Chronic exercise ameliorated HFD-triggered hepatic injury and down-regulated pro-inflammatory mediator levels. Liver H & E stained sections showed that 12-week administration of HFD induced typical NASH pathological phenotypes, which included large lipid droplet accumulation, infiltration of inflammatory cells and necrosis of hepatocytes, while treatment with exercise reversed the hepatic histopathological features and exhibited cellular architecture comparable to the control rats (Fig. 4A). The NASH scoring (Fig. 4B) also supported this finding which was consistent with our previous work (Xiao et al., 2013). Consistently, the serum ALT level of HFD group was significantly upregulated, which was markedly reduced by chronic exercise (Fig. 4C). The development of NASH significantly upregulated the mRNA level of pro-inflammatory mediators TNF-α and IL-1β which were alleviated by exercise (Fig. 4D,E). A similar trend was also observed for the master inflammatory regulator, nuclear transcription factor NF-ϰB (Fig. 4F), suggesting the anti-inflammatory effect of chronic exercise.

Chronic aerobic exercise attenuated oxidative stress triggered apoptosis

The formation of lipid peroxidation product MDA was measured in each group of rats. NASH induced by HFD enhanced MDA formation, which was significantly reduced by exercise training (Fig. 5A). In contrast, the mRNA level of antioxidant enzymes catalase (CAT) and glutathione peroxidase (GPx) were markedly down-regulated by the induction of HFD, but was significantly restored by exercise, indicating the antioxidant effect of chronic aerobic exercise (Fig. 5B,C). As a key mediator which regulated the production of reactive oxygen species, CYP2E1 expression level was sharply elevated in HFD group and it was markedly reduced by chronic exercise to the basal expression level (Fig. 5D,E).

To study the effect of physical exercise on the downstream hepatic apoptosis, protein expressions of key apoptotic pathways, including BAX, cleaved caspase-3, and cleaved PARP were measured by western blot. The expression levels of BAX, cleaved caspase-3, and cleaved PARP were upregulated during NASH induced by HFD, which was significantly reduced after exercise (Fig. 5D,F-H, respectively). As an essential intrinsic mediator in apoptosis, cytochrome c, was released from mitochondria to cytoplasm during NASH development. Co-treatment with chronic exercise further

increased cytochrome c level only in the mitochondria, but not in the cytoplasmic fractions, suggesting the induction of mitophagy by exercise to digest the damaged component caused by HFD. VDAC acted as a housekeeping marker which was constantly expressed in mitochondria (Fig. 5I). TUNEL results also verified the similar findings in apoptosis but not mitophagy (Fig. 6A), and the statistical analysis is shown in Fig. 6B.

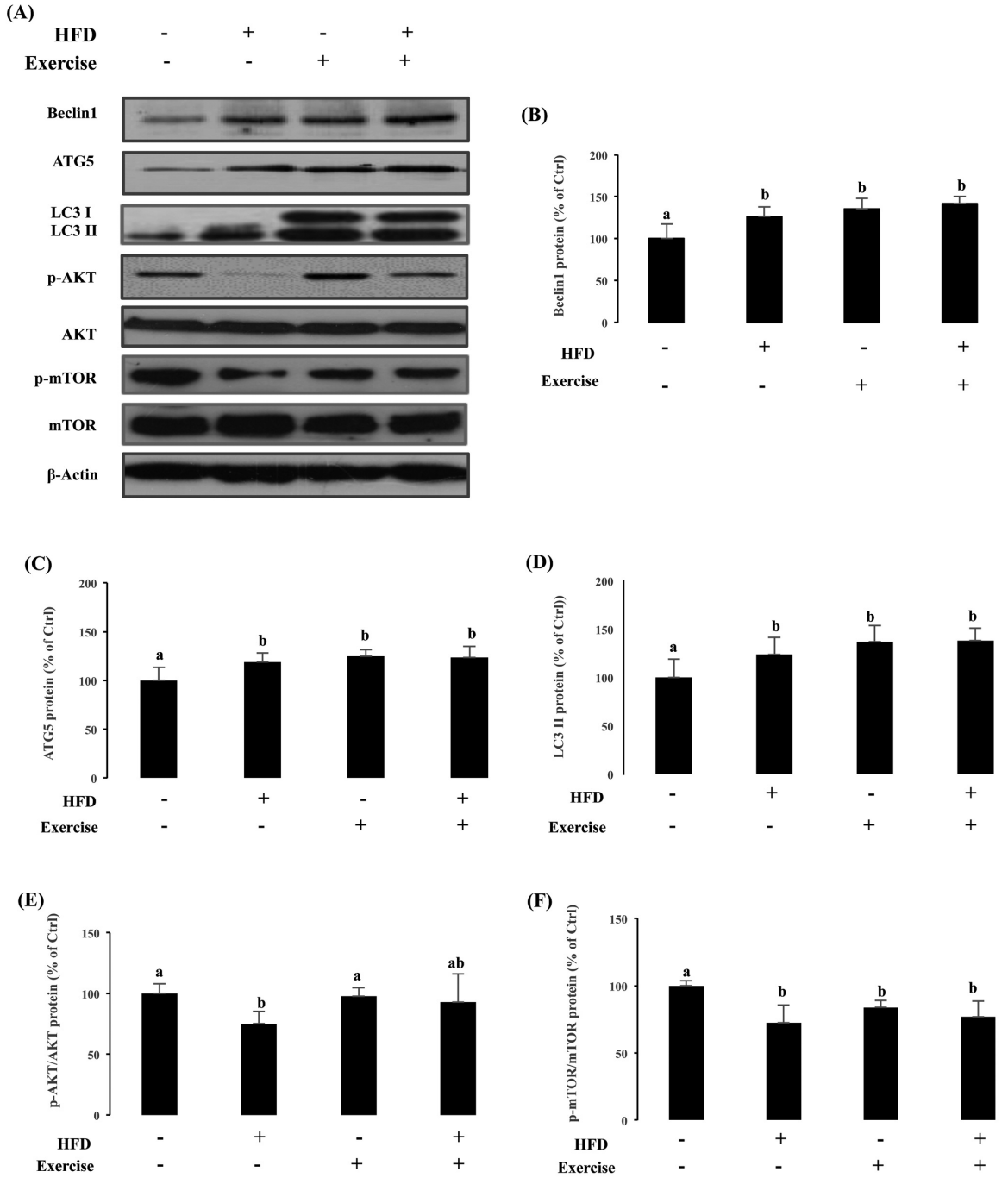

Fig. 1. Chronic exercise induced cytoprotective autophagy via the inhibition of AKT/mTOR pathway in NASH induced by HFD. Western blot results of the expressional changes of Beclin1, ATG5, LC3, p-AKT, AKT, p-mTOR and mTOR **(A)**, and statistical analysis for Beclin1 **(B)**, ATG5 **(C)**, LC3II **(D)**, p-AKT/AKT **(E)**, and p-mTOR/mTOR **(F)** are shown. Data presented are expressed as Mean ± SD (n=6) and experimental groups without a common letter above the bar histograms are significantly different ($p<0.05$).

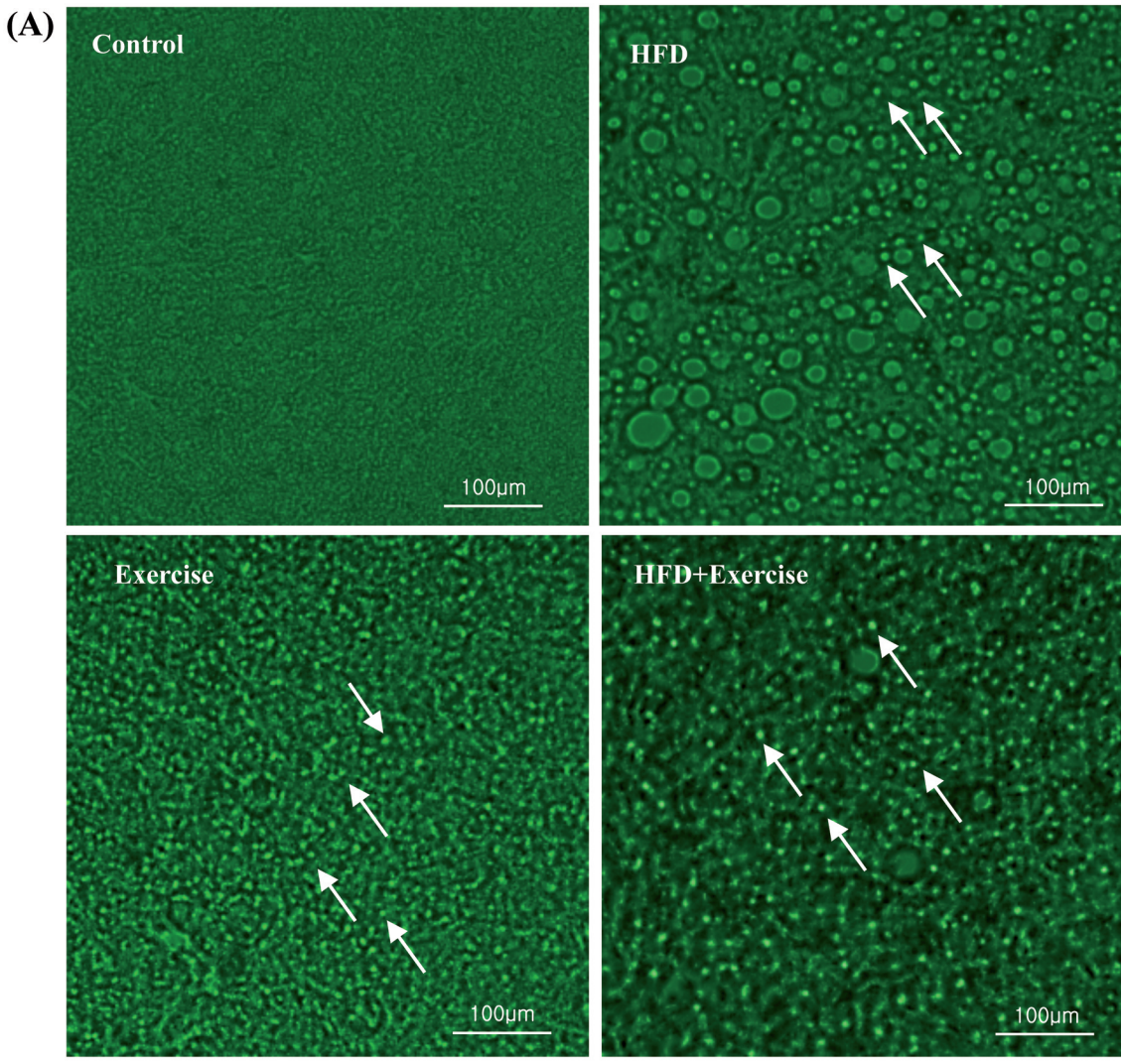

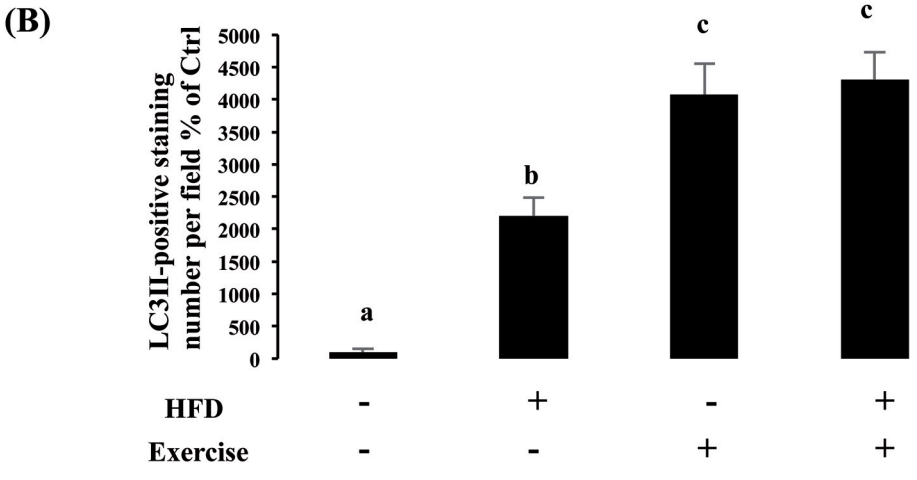

Fig. 2. LC3 aggregation was quantified under fluorescence microscope after immuno-staining. Bright green dots indicated by arrows are under the field of microscope **(A),** and the statistical analysis is shown in **(B)**. Data presented are expressed as Mean ± SD (n=6) and experimental groups without a common letter above the bar histograms are significantly different ($p<0.05$).

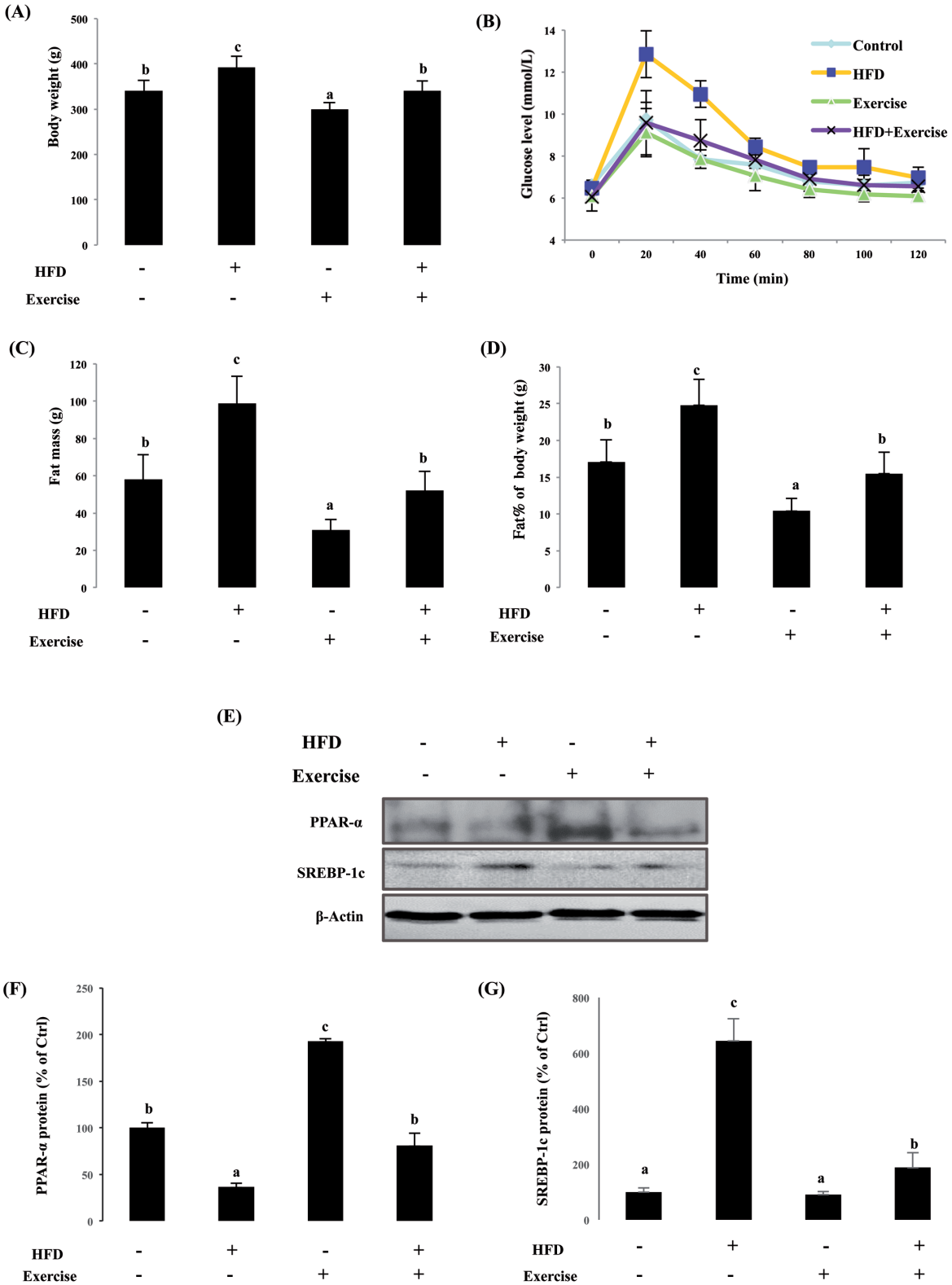

Fig. 3. Chronic exercise mitigated HFD-induced lipid accumulation and glucose metabolism dysfunction during NASH progression. The relevant data were tested including body weight **(A)**, GTT **(B)**, fat mass **(C)**, fat composition **(D)**, and the western blot results of PPAR-α and SREBP-1c **(E)**, as well as the statistical analysis for PPAR-α **(F)** and SREBP-1c **(G)**, respectively. Data presented are expressed as Mean ± SD (n=6) and experimental groups without a common letter above the bar histograms are significantly different ($p<0.05$).

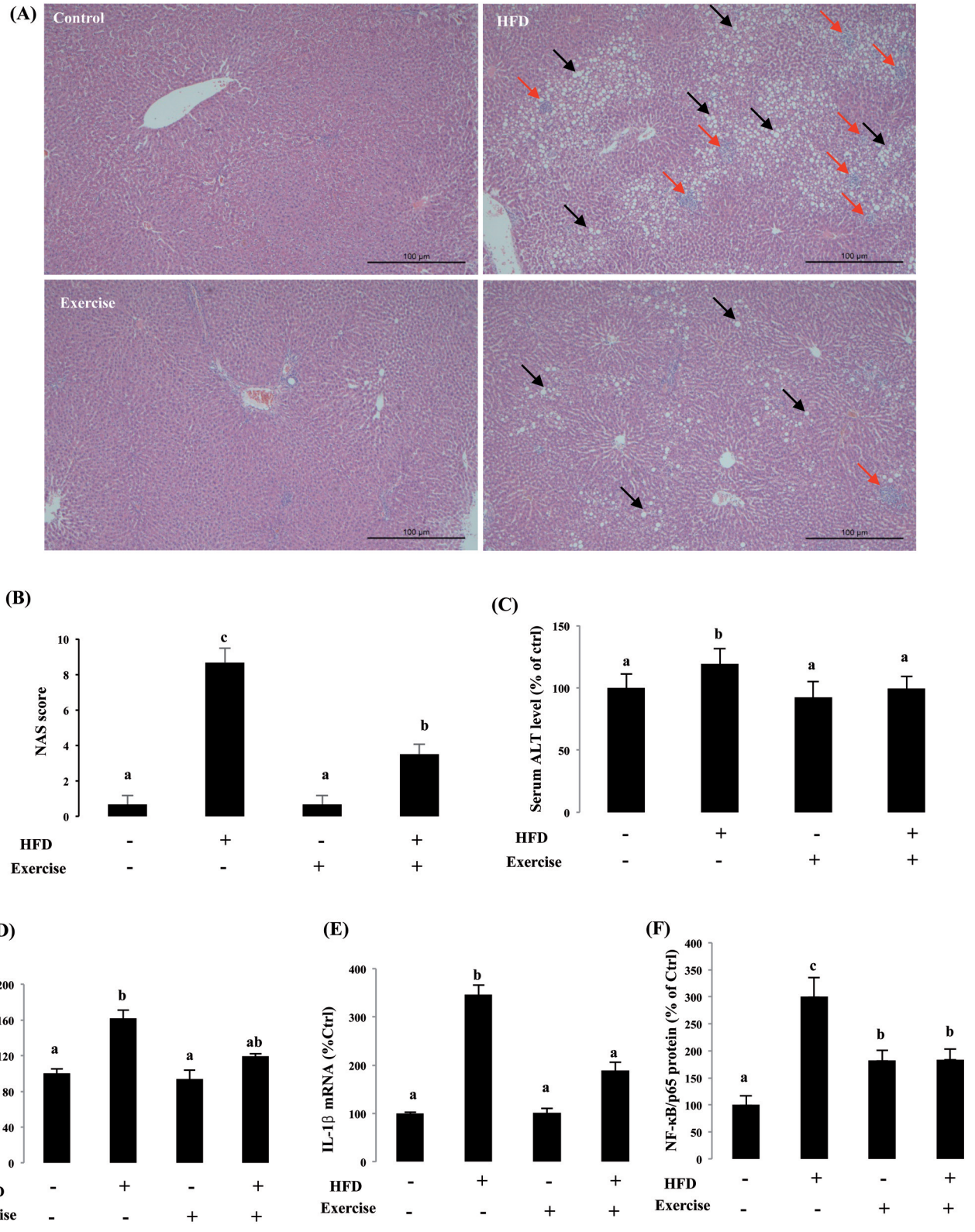

Fig. 4. Chronic exercise attenuated NASH-mediated hepatic injury and decreased the levels pro-inflammatory mediators. H&E staining **(A)** of rat liver on Control, HFD treatment, Exercise treatment, and HFD+Exercise groups (Mag.= 200x), NAS score **(B)**, serum ALT level **(C)**, mRNA expression levels for TNF-α (**D)** and IL-1β **(E),** and the protein level of nuclear transcription factor NF-κB **(F)** by ELISA were evaluated. Typical hepatic fat accumulations were indicated by black arrows and inflammatory infiltrates were labeled with red arrows. Data presented are expressed as Mean ± SD (n=6) and experimental groups without a common letter above the bar histograms are significantly different ($p<0.05$).

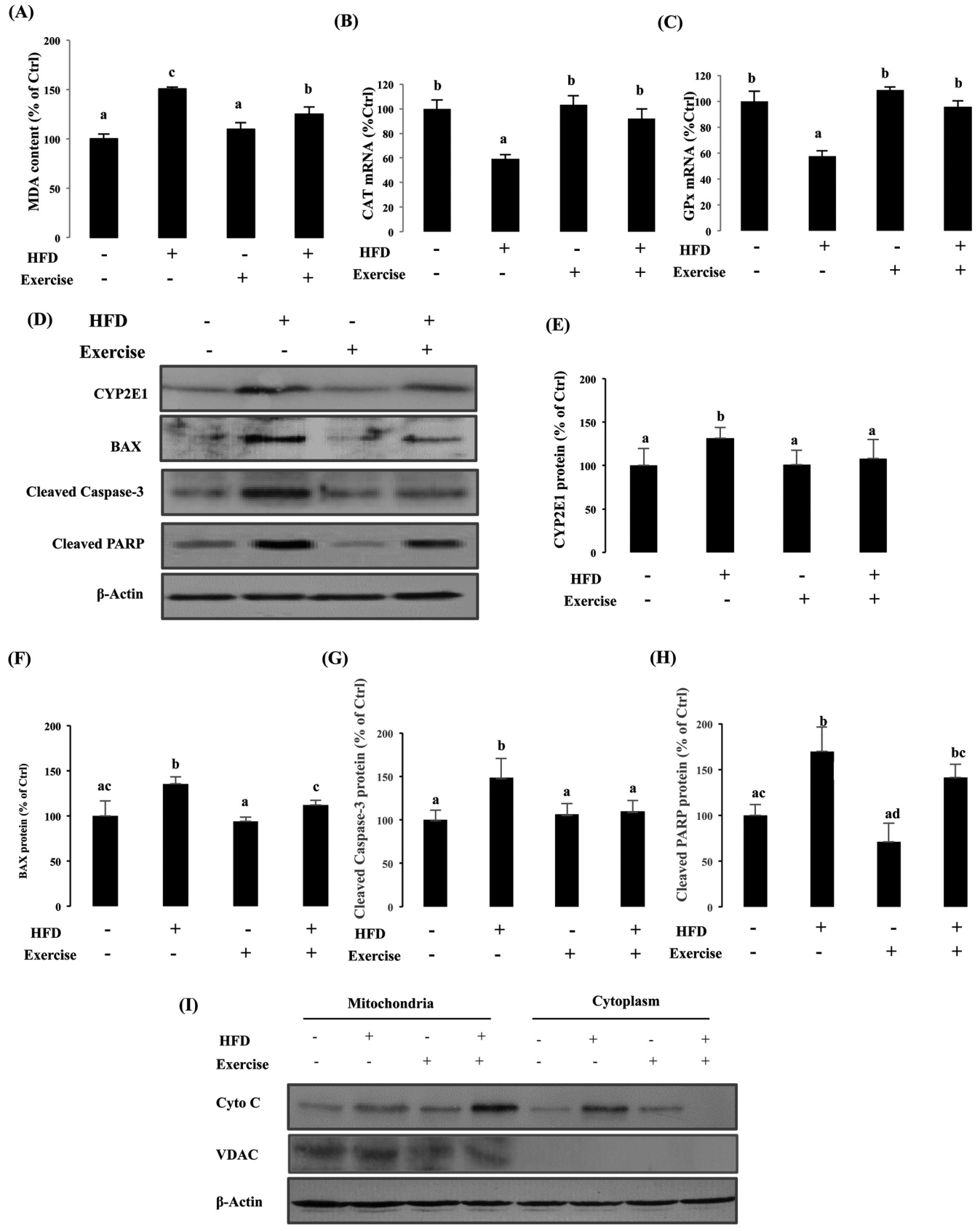

Fig. 5. Chronic exercise ameliorated oxidative stress triggered apoptosis through mitochondrial dependent pathway in NASH induced by HFD. Ameliorative effect of exercise on lipid peroxidation by MDA assay **(A)**, mRNA expression levels of CAT **(B)** and GPx **(C)**, western blot results of the expressional changes of CYP2E1, BAX, cleaved caspase-3, and cleaved PARP **(D)**, as well as the statistical analysis for CYP2E1 **(E)**, BAX **(F)**, cleaved caspase-3 **(G)**, and cleaved PARP **(H)** were tested. In addition, western blot for an accumulation of cytochrome c (Cyto c) in both mitochondrial and cytoplasmic fractions were also detected **(I)**. Data presented are expressed as Mean ± SD (n=6) and experimental groups without a common letter above the bar histograms are significantly different ($p<0.05$).

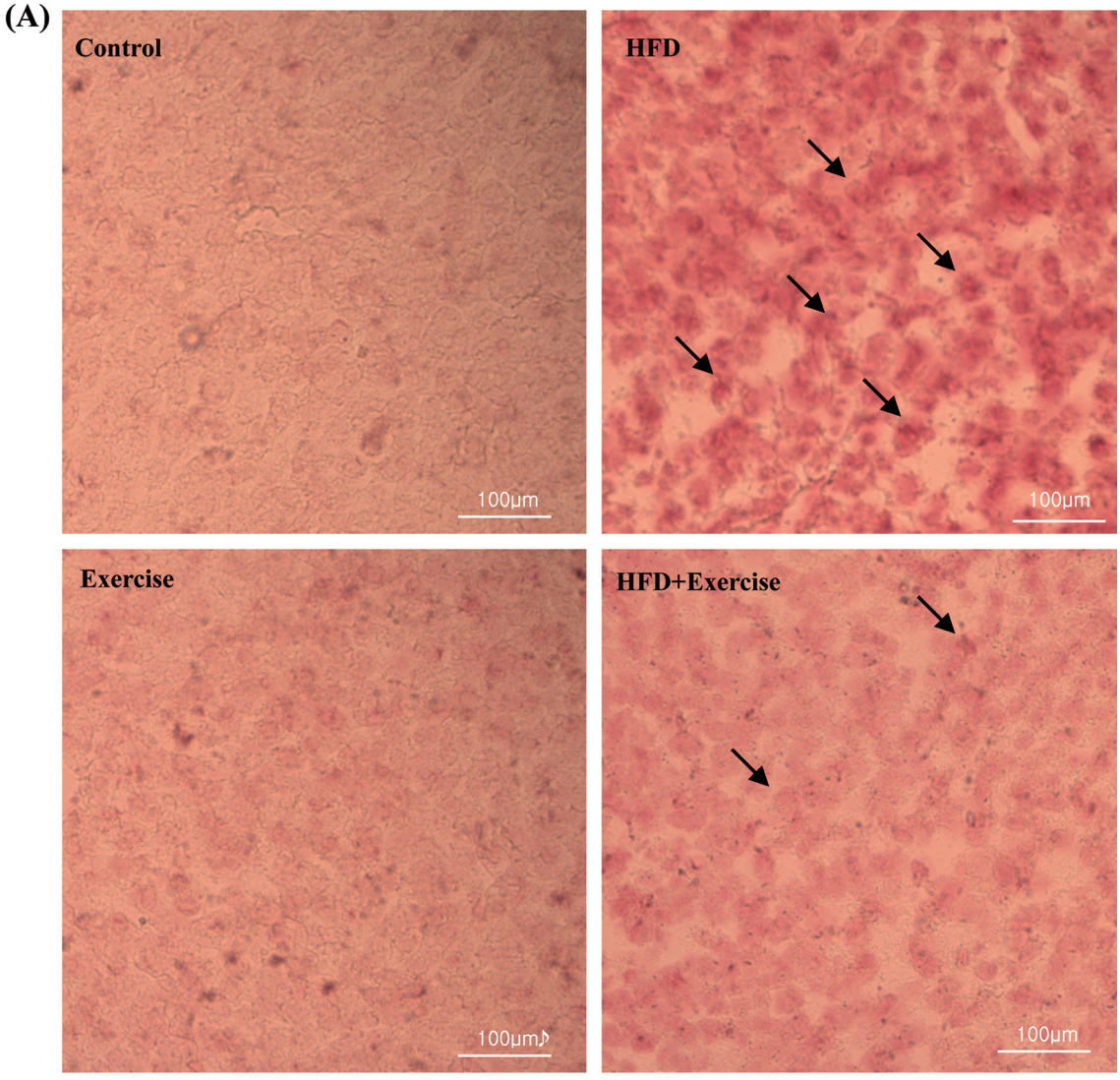

Fig. 6. TUNEL staining for rat liver is shown in **(A)**, and summary of data and statistical result is shown in **(B)**. TUNEL events were pointed out with black arrows. Data presented are expressed as Mean ± SD (n=6) and experimental groups without a common letter above the bar histograms are significantly different ($p<0.05$).

Physical training ameliorated NASH-mediated lysosomal membrane permeabilisation and cathepsin B activation.

Lysosomal reaction could initiate programmed cell death by necrosis, apoptosis, autophagy and a modification of lysosomal membrane permeability, which is considered a key early event in the lysosomal cell death pathway (Wu et al., 2013). Lysosomal membrane protein, LAMP1, was mainly collected in membrane protein fractions. Both NASH induced by HFD and exercise treatment enhanced the expression level of LAMP1 compared with the control group. β-actin and COX IV served as housekeeping markers which were expressed in cytosol and membrane fractions respectively. Interestingly, LAMP1 was not detected in the cytosolic fractions of HFD group samples suggesting that NASH development did not cause lysosomal membrane disruption and release of LAMP1 into the cytosolic compartment (Fig. 7A). Hoegen demonstrated that it was the lysosomal membrane destabilisation, but not disruption that triggered cathepsin B released from lysosome to cytosol to participate in cell programming pathways (Hoegen et al., 2011). It has been reported that lysosomal membrane destabilisation was mainly achieved by inducing ROS to peroxidase membrane lipids, which caused the high concentration of extracellular ATP, ultimately leading to lysosome destabilisation and cathepsin B release (Lopez-Castejon et al., 2010). As shown in Fig. 7B, NASH induced by HFD significantly increased cathepsin B expression level which was down-regulated by exercise training in the co-treatment group. A similar trend was also observed in cathepsin B activity test (Fig. 7C), which was also consistent with that of apoptotic markers and inflammatory mediators, further suggesting that the release of cathepsin B into the cytosol may play an important role in the induction of NASH.

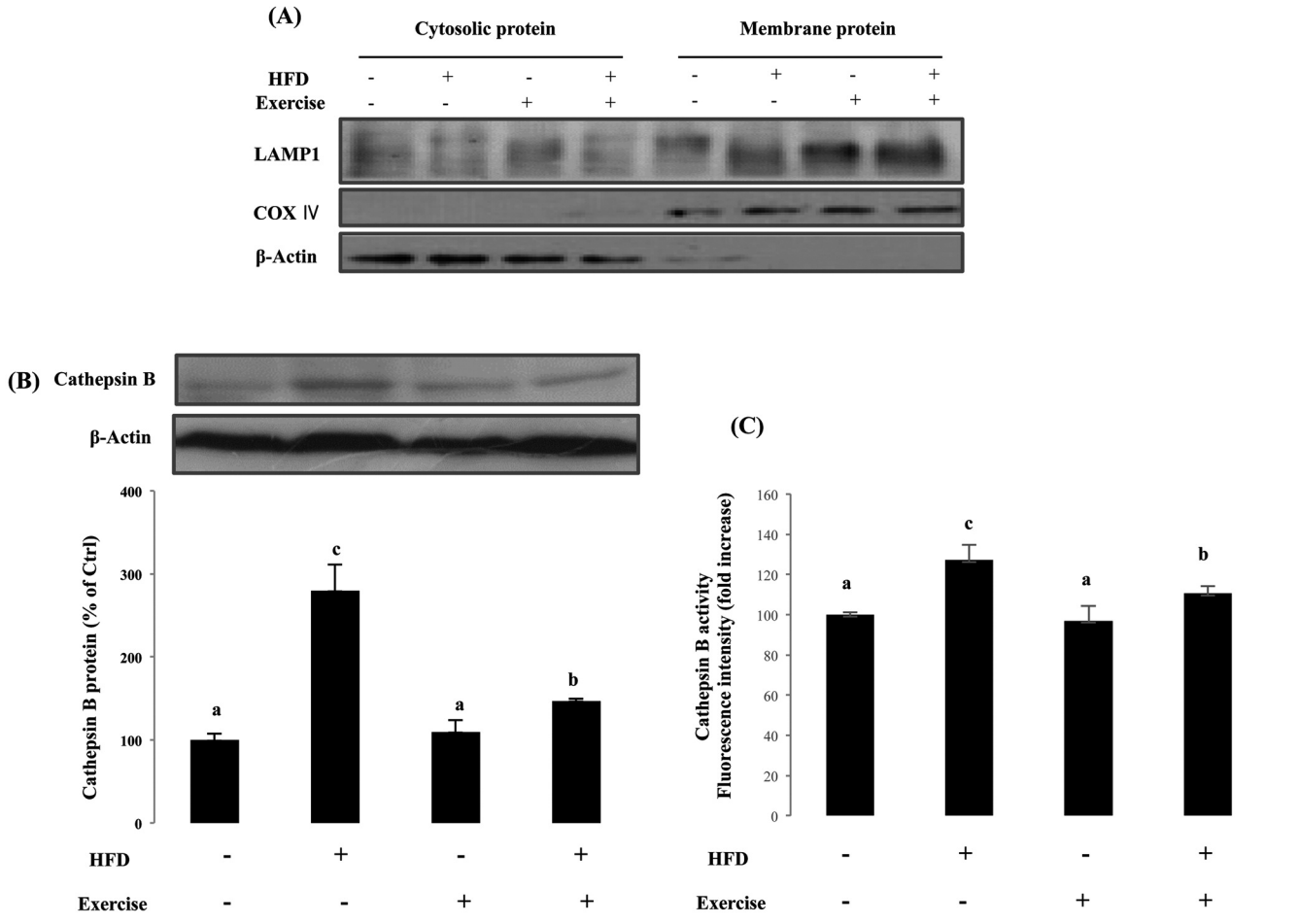

Fig. 7. Chronic exercise diminished ROS-triggered lysosomal membrane permeabilisation and cathepsin B activation during NASH development. Western blots for LAMP1 in both cytosolic and membrane fractions **(A),** as well as cathepsin B protein level **(B)** and activity **(C)** were evaluated. Data presented are expressed as Mean ± SD (n=6) and experimental groups without a common letter above the bar histograms are significantly different ($p<0.05$).

Discussion

Autophagy is considered as a newly defined cellular process which exerts beneficial effects on NASH, including reducing triglyceride and cholesterol levels, improving insulin homeostasis, mitigating hepatic oxidative stress, diminishing TNF mediated liver inflammation, and decreasing the risk of developing hepatic carcinoma (Gonzalez-Rodriguez et al., 2014). A significant increase in LC3II level was detected in patients with NASH as compared to subjects with a normal liver (Grumati et al., 2010), suggesting the activation of autophagy as a self-protective mechanism in NASH. Exercise improves glucose metabolism in mice and induces cytoprotective autophagy (He et al., 2012). Additionally, physical exercise stimulates autophagy in skeletal muscle, which exerts positive effects on maintaining tissue homeostasis by removing dysfunctional mitochondria (Grumati et al., 2010). Marques-Aleixo's group demonstrated that physical activity elevated the level of autophagy markers, resulting in the increased content of Beclin1 and LC3II in the brain cortex and cerebellum (Marques-Aleixo et al., 2015). As shown in Figs. 1, 2, both NASH induced by HFD and exercise training elevated the expression levels of autophagy markers Beclin1, ATG5, and LC3II. However, in the co-treatment group, they did not exhibit synergistic effects but maintained elevated levels of autophagy markers. These findings suggested that a) autophagy induced during NASH progression played a cytoprotective role in the removal of damaged components for cell survival, and b) chronic exercise ameliorated HFD-triggered NASH and maintained hepato-protective autophagy.

For the upstream pathway, it has been shown that inhibition of negative autophagic regulator mTOR by rapamycin down-regulated oleic acid-TG accumulation in fatty liver mouse model (Guillaud-Bataille et al., 2009). In this study, physical training induced hepato-protective autophagy by decreasing the level of p-mTOR. This finding suggested that autophagy induction was mainly achieved through the inhibition of mTOR activity characterised by the reduction of mTOR phosphorylation. Interestingly, as the upstream of mTOR, p-AKT did not exhibit a similar expression trend as p-mTOR, which indicated that p-AKT may participate in other signaling pathways such as oxidative stress and apoptosis. It has been reported that p-AKT inhibited apoptosis induced by damage-regulated autophagy modulator (DRAM)-mediated mitophagy in hepatocellular carcinoma by preventing the translocation of DRAM to mitochondria (Suzuki et al., 2014). Additionally, the cardio-protection of hyperoxide preconditioning against MIRI may be related to the activation of PI3K/Akt signaling pathway with upregulation of BCL-2 and downregulation of Bax (Han et al., 2015), indicating that p-AKT may play a crucial role in the cross-talk between autophagy and apoptosis networks serving as a positive regulator in facilitating cell survival. We concur that AKT pathway may also regulate inflammation and fibrosis. However, our data showed that the p-AKT protein in exercise group was higher than HFD group with a basal level similar to the control. TNF-α, IL-1β and NASH scoring also showed that the exercise group had a basal level similar to the control group whereas the HFD group had the highest level including NF-ϰB expression. Taken together, our data seem to suggest that p-AKT pathway may not play a dominant role in inflammation and fibrosis and these processes were partly induced by NF-ϰB activation and pathway.

Lipophagy is defined as the sequestration of lipid droplets by autophagosomes and their degradation within the lysosome (Singh and Cuervo, 2012). Autophagy inhibition aggravates hepatocellular lipid accumulation while autophagy activation plays an essential role in the clearance of hepatic lipid droplets (Martinez-Lopez and Singh, 2015). This implies that the induction of lipophagy can serve as a strategy to rapidly mobilise liver cell lipids and reduce lipid accumulation within lipid droplets. As shown in Fig. 3, the body weight, fat mass and fat composition were markedly reduced, β-oxidation regulator PPAR-α was significantly upregulated, and the level of fatty acid synthesis marker SREBP-1c was markedly decreased after chronic exercise. Taken together, lipophagy induced by exercise exerted beneficial effects on mitigating lipid accumulation by breaking down the lipid droplets into free fatty acid, allowing it to take part in fatty acid oxidation process to generate energy for body metabolism. Lipophagy also contributed to the inhibition of NASH progression by reducing lipid accumulation.

Cathepsin B, which is located in the lysosome, plays an essential role in heterophagic and autophagic processes to maintain the homeostasis of the cell metabolism (Cesen et al., 2012; Goyal et al., 2015). Following the targeted lysosomal membrane destabilisation, cathepsin B will be released from the lysosome to the cytosol to initiate a series of lysosome-associated signaling pathways such as inflammation and apoptosis (Feng et al., 2013). In this study, we observed that the lysosomal associated membrane protein, LAMP1, was mainly detected in the membrane protein fraction rather than cytosolic protein fraction of HFD group samples. This suggests that the progression of NASH did not result in lysosomal membrane disruption, leading to lysosomal membrane break and LAMP1 being released into the cytosol (Fig. 7A). It has been reported that the translocation of cathespin B from the lysosome to the cytosol was based on lysosomal membrane destabilisation, but not membrane disruption (Hoegen et al., 2011). Furthermore, lysosomal membrane destabilisation was mainly achieved by inducing ROS to peroxidase membrane lipids (Lopez-Castejon et al., 2010). Under oxidative stress conditions, huge amounts of hydrogen peroxides are generated in the mitochondria which could not be completely detoxified, leading to its diffusion into their permeable

lysosomes (Kurz et al., 2008). The acidic pH and the high iron content facilitate a Fenton-type of reaction to generate more highly reactive hydroxyl radicals, ultimately contributing to peroxidation of membrane lipids and lysosome destabilisation-mediated cathepsin B release (Cesen et al., 2012). In our study, HFD increased the level of CYP2E1 followed by ROS generation. However, chronic exercise training showed an obvious antioxidant activity by significantly down-regulating CYP2E1 expression level to reduce ROS (Fig. 5E). This effect was further facilitated by the restoration of antioxidant enzymes CAT and GPx and inhibited lipid peroxidation end product MDA. As a result, the antioxidant effect of physical exercise eventually inhibited the process of lysosome membrane destabilisation and cathepsin B released into the cytosol, which may facilitate the fusion with autophagosome and to induce cytoprotective autophagy.

Cathepsin B is already active when released into the cytosol following lysosomal membrane permeabilisation to interact with other proteins in order to participate in cell signaling pathways such as inflammation and apoptosis (Turk and Stoka, 2007). Guicciardi showed that cathepsin B played a critical role in TNF-α related liver injury (Guicciardi et al., 2001). Another report demonstrated that lysosomal permeabilisation accompanied by the release of cathepsin B contributed to IL-1β secretion. Then IL-1β can further bind to the NLRP-3 inflammasome, causing caspase-1 activation, finally leading to the induction of inflammation-mediated pathways (Bruchard et al., 2013). Similar findings showed that NLRP-3 inflammasome was activated through ATP-dependent lysosomal permeabilisation and cathepsin B release, finally leading to brain injury in pneumococcal meningitis (Lopez-Castejon et al., 2010). In our study, NASH progression markedly elevated TNF-α and IL-1β levels, which exhibited a similar trend to that of cathepsin B (Fig. 7B,C), indicating that the released cathepsin B, after lysosomal permeabilisation, may play an essential role in the regulation of hepatic inflammation by interacting with pro-inflammatory mediators. In contrast, physical exercise diminished such inflammatory processes by down-regulating TNF-α, IL-1β and cathepsin B expression levels, as well as cathepsin B activity, which suggested that the ameliorative effect of exercise was partially achieved through both the down-regulation of cathepsin B expression and the inhibition of cytosolic cathepsin B activity.

Cathepsin B could also serve as an amplifier of apoptotic signaling. The cathepsin B released from lysosomes has been shown to process BID and degrade the anti-apoptotic Bcl-2 proteins, which further activated pro-apoptotic protein BAX to trigger mitochondria-dependent apoptosis (Droga-Mazovec et al., 2008). In this study, CYP2E1 was catalysed to produce ROS, which downregulated the expression of antioxidant enzymes CAT and GPx and promoted lipid peroxidation end product MDA level to trigger oxidative stress (Fig. 5A-C). On one hand, the existing oxidative stress can trigger self-mediated mitochondria-dependent apoptosis through cytochrome c release from the mitochondria to the cytosol as well as activating key apoptotic markers, including BAX, cleaved caspase-3, and cleaved PARP (Fig. 5D,I). One the other hand, ROS can oxidise membrane lipids leading to lysosome membrane destabilisation and cathepsin B release. Then, cathepsin B in cytosol can further interact with Bcl-2 family members to amplify mitochondria-associated apoptotic signaling. Physical training dramatically decreased CYP2E1 level to mitigate ROS production. This attenuated the downstream apoptosis by down-regulating apoptotic markers, and also blocked the process of cathepsin B released into the cytosol by mitigating the oxidation of the lysosomal membrane lipids. Thus, chronic exercise played dual beneficial roles, including diminishing the apoptotic cell death through the mitochondria-dependent pathway, and keeping the lysosomal membrane stable to facilitate the liver cells to undergo the cytoprotective autophagic process.

In conclusion, cytoprotective autophagy was induced as a self-protective mechanism during NASH development. Chronic exercise therapeutically mitigated NASH-mediated oxidative stress, inflammation and apoptosis partly by inducing the hepato-protective autophagy. The signaling pathway during NASH progression involved ROS generated by CYP2E1, which might cause the oxidation of the lysosomal membrane lipids and may possibly lead to lysosomal destabilisation and cathepsin B release into the cytosol. Cathepsin B participated in inflammatory pathways and amplified mitochondria-dependent apoptotic cell death. Chronic exercise, on the contrary, remarkably decreased ROS production by down-regulating CYP2E1 level, which might contribute to the inhibition of lysosomal membrane permeabilisation and cathepsin B release. This may facilitate the fusion of lysosome and autophagosome to complete the cytoprotective autophagic process, and diminish the cathespin B-dependent inflammatory and apoptotic process, ultimately resulting in the improvement of NASH pathological features.

Acknowledgements. We would like to thank Ms. Carman Leung for her technical help in this project. This study is partly supported by Seed fund for Basic Research (201611159263), University Research Committee, The University of Hong Kong.

The authors' contributions are as follows: RG and GLT mainly designed the experiments; ECL, MLF helped design; RG and YQ conducted the experiments; RG, YQ and GLT analysed data, performed statistical tests and wrote the manuscript; all reviewed the final version of the manuscript.

Conflict of interest. We do not have any professional relationships with companies or manufacturers who will benefit from the results of the present study. We declare that the results of the study are presented clearly, honestly, and without fabrication, falsification, or inappropriate data manipulation.

References

Alkhouri N., Carter-Kent C and Feldstein A.E. (2011). Apoptosis in nonalcoholic fatty liver disease: diagnostic and therapeutic implications. Expert. Rev. Gastroenterol. Hepatol. 5, 201-212.

Amir M. and Czaja M.J. (2011). Autophagy in nonalcoholic steatohepatitis. Expert. Rev. Gastroenterol. Hepatol. 5, 159-166.

Bruchard M., Mignot G., Derangère V., Chalmin F., Chevriaux A., Vegran F., Boireau W., Simon B., Ryffel B., Connat J.L., Kanellopoulos J., Martin F., Rebe C., Apetoh L. and Ghiringhelli F. (2013). Chemotherapy-triggered cathepsin B release in myeloid-derived suppressor cells activates the Nlrp3 inflammasome and promotes tumor growth. Nat. Med. 19, 57-64.

Cesen M.H., Pegan K., Spes A. and Turk B. (2012). Lysosomal pathways to cell death and their therapeutic applications. Exp. Cell Res. 318, 1245-1251.

Droga-Mazovec G., Bojic L., Petelin A., Ivanova S., Romih R., Repnik U., Salvesen G.S., Stoka V., Turk V. and Turk B. (2008). Cysteine cathepsins trigger caspase-dependent cell death through cleavage of bid and antiapoptotic Bcl-2 homologues. J. Biol. Chem. 283, 19140-19150.

Feng Y., Ni L. and Wang Q. (2013). Administration of cathepsin B inhibitor CA-074Me reduces inflammation and apoptosis in polymyositis. J. Dermatol. Sci. 72, 158-167.

Gonzalez-Rodriguez A., Mayoral R., Agra N., Valdecantos M.P., Pardo V., Miquilena-Colina M.E., Vargas-Castrillon J., Lo Iacono O., Corazzari M., Fimia G.M., Piacentini M., Muntané J., Bosca L., Garcia-Monzon C., Martin-Sanz P. and Valverde A.M. (2014). Impaired autophagic flux is associated with increased endoplasmic reticulum stress during the development of NAFLD. Cell Death Dis. 5, e1179.

Goyal S., Amar S.K., Dubey D., Pal M.K., Singh J., Verma A., Kushwaha H.N. and Ray R.S. (2015). Involvement of cathepsin B in mitochondrial apoptosis by p-phenylenediamine under ambient UV radiation. J. Hazard Mater. 300, 415-425.

Grumati P., Coletto L., Sabatelli P., Cescon M., Angelin A., Bertaggia E., Blaauw B., Urciuolo A., Tiepolo T., Merlini L., Maraldi N.M., Bernardi P., Sandri M. and Bonaldo P. (2010). Autophagy is defective in collagen VI muscular dystrophies, and its reactivation rescues myofiber degeneration. Nat. Med. 16, 1313-1320.

Guicciardi M.E., Miyoshi H., Bronk S.F. and Gores G.J. (2001). Cathepsin B knockout mice are resistant to tumor necrosis factor-alpha-mediated hepatocyte apoptosis and liver injury: implications for therapeutic applications. Am. J. Pathol. 159, 2045-2054.

Guillaud-Bataille M., Brison O., Danglot G., Lavialle C., Raynal B., Lazar V., Dessen P. and Bernheim A. (2009). Two populations of double minute chromosomes harbor distinct amplicons, the MYC locus at 8q24.2 and a 0.43-Mb region at 14q24.1, in the SW613-S human carcinoma cell line. Cytogenet. Genome Res. 124, 1-11.

Guo R., Liong E.C., So K.F., Fung M.L. and Tipoe G.L. (2015). Beneficial mechanisms of aerobic exercise on hepatic lipid metabolism in non-alcoholic fatty liver disease. Hepatobiliary Pancreat Dis. Int. 14, 139-144.

Han J., Xuan J.L., Hu H.R. and Chen Z.W. (2015). Protective effect against myocardial ischemia reperfusion injuries induced by hyperoside preconditioning and its relationship with PI3K/Akt signaling pathway in rats. Zhongguo Zhong Yao Za Zhi. 40, 118-123 (In Chinese).

He C., Bassik M.C., Moresi V., Sun K., Wei Y., Zou Z., An Z., Loh J., Fisher J., Sun Q., Korsmeyer S., Packer M., May H.I., Hill J.A., Virgin H.W., Gilpin C., Xiao G., Bassel-Duby R., Scherer P.E. and Levine B. (2012). Exercise-induced BCL2-regulated autophagy is required for muscle glucose homeostasis. Nature 481, 511-515.

Hoegen T., Tremel N., Klein M., Angele B., Wagner H., Kirschning C., Pfister H.W., Fontana A., Hammerschmidt S. and Koedel U. (2011). The NLRP3 inflammasome contributes to brain injury in pneumococcal meningitis and is activated through ATP-dependent lysosomal cathepsin B release. J. Immunol. 187, 5440-5451.

Kim Y.A., Kim Y.S., Oh S.L., Kim H.J. and Song W. (2013). Autophagic response to exercise training in skeletal muscle with age. J. Physiol. Biochem. 69, 697-705.

Kleiner D.E., Brunt E.M., Van Natta M., Behling C., Contos M.J., Cummings O.W., Ferrell L.D., Liu Y.C., Torbenson M.S., Unalp-Arida A., Yeh M., McCullough A.J. and Sanyal A.J. (2005). Design and validation of a histological scoring system for nonalcoholic fatty liver disease. Hepatology 41, 1313-1321.

Kurz T., Terman A., Gustafsson B. and Brunk U.T. (2008). Lysosomes and oxidative stress in aging and apoptosis. Biochim. Biophys. Acta 1780, 1291-1303.

Lavallard V.J. and Gual P. (2014). Autophagy and non-alcoholic fatty liver disease. Biomed. Res. Int. 120179.

Lopez-Castejon G., Theaker J., Pelegrin P., Clifton A.D., Braddock M. and Surprenant A. (2010). P2X(7) receptor-mediated release of cathepsins from macrophages is a cytokine-independent mechanism potentially involved in joint diseases. J. Immunol. 185, 2611-2619.

Loyer X., Paradis V., Henique C., Vion A.C., Colnot N., Guerin C.L., Devue C., On S., Scetbun J., Romain M., Paul J.L., Rothenberg M.E., Marcellin P., Durand F., Bedossa P., Prip-Buus C., Bauge E., Staels B., Boulanger C.M., Tedgui A. and Rautou P.E. (2016). Liver microRNA-21 is overexpressed in non-alcoholic steatohepatitis and contributes to the disease in experimental models by inhibiting PPARalpha expression. Gut 65, 1882-1894.

Marques-Aleixo I., Santos-Alves E., Balca M.M., Rizo-Roca D., Moreira P.I., Oliveira P.J., Magalhaes J. and Ascensao A. (2015). Physical exercise improves brain cortex and cerebellum mitochondrial bioenergetics and alters apoptotic, dynamic and auto(mito)phagy markers. Neuroscience 301, 480-495.

Martinez-Lopez N. and Singh R. (2015). Autophagy and Lipid Droplets in the Liver. Annu. Rev. Nutr. 35, 215-237.

Puri P. and Chandra A. (2014). Autophagy modulation as a potential therapeutic target for liver diseases. J. Clin. Exp. Hepatol. 4, 51-59.

Singh R. and Cuervo A.M. (2012). Lipophagy: connecting autophagy and lipid metabolism. Int. J. Cell Biol. 2012, 282041.

Suzuki N., Yoneda M., Tanabe K., Fujimoto A., Iha K., Seno K., Yamada K., Iwamoto T., Masuo Y. and Hirofuji T. (2014). Lactobacillus salivarius WB21--containing tablets for the treatment of oral malodor: a double-blind, randomized, placebo-controlled crossover trial. Oral Surg. Oral Med. Oral Pathol. Oral Radiol. 117, 462-470.

Tipoe G.L., Leung T.M., Liong E., So H., Leung K.M., Lau T.Y., Tom W.M., Fung M.L., Fan S.T. and Nanji A.A. (2006). Inhibitors of inducible nitric oxide (NO) synthase are more effective than an NO donor in reducing carbon-tetrachloride induced acute liver injury. Histol. Histopathol. 21, 1157-1165.

Tipoe G.L., Ho C.T., Liong E.C., Leung T.M., Lau T.Y., Fung M.L. and Nanji A.A. (2009). Voluntary oral feeding of rats not requiring a very high fat diet is a clinically relevant animal model of non-alcoholic fatty liver disease (NAFLD). Histol. Histopathol. 24, 1161-1169.

Turk B. and Stoka V. (2007). Protease signalling in cell death: caspases versus cysteine cathepsins. FEBS Lett. 581, 2761-2767.

Wu M., Ming W., Tang Y., Zhou S., Kong T. and Dong W. (2013). The anticancer effect of cytotoxin 1 from Naja atra Cantor venom is mediated by a lysosomal cell death pathway involving lysosomal membrane permeabilization and cathepsin B release. Am. J. Chin Med. 41, 643-663.

Xiao J., Guo R., Fung M.L., Liong E.C., Chang R.C., Ching Y.P. and Tipoe G.L. (2013). Garlic-derived S-allylmercaptocysteine ameliorates nonalcoholic fatty liver disease in a rat model through inhibition of apoptosis and enhancing autophagy. Evid. Based Complement. Alternat. Med. 2013, 642920.

Accepted January 24, 2020